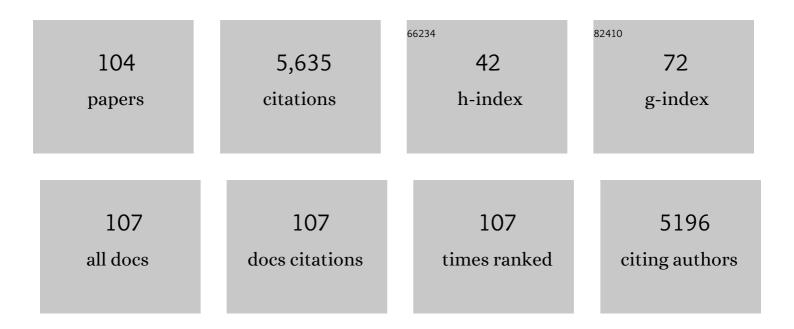


## List of Publications by Year in descending order

Source: https://exaly.com/author-pdf/4876273/publications.pdf Version: 2024-02-01



LIANC LL

#	Article	IF	CITATIONS
1	CMOS ompatible Electronic–Plasmonic Transducers Based on Plasmonic Tunnel Junctions and Schottky Diodes. Small, 2022, 18, e2105684.	5.2	9
2	The Unusual Dielectric Response of Large Area Molecular Tunnel Junctions Probed with Impedance Spectroscopy. Advanced Electronic Materials, 2022, 8, 2100495.	2.6	10
3	Preventing the Capillary-Induced Collapse of Vertical Nanostructures. ACS Applied Materials & Interfaces, 2022, 14, 5537-5544.	4.0	7
4	Spatial Control over Stable Lightâ€Emission from ACâ€Driven CMOSâ€Compatible Quantum Mechanical Tunnel Junctions. Laser and Photonics Reviews, 2022, 16, .	4.4	7
5	Improving Orientation, Packing Density, and Molecular Arrangement in Self-Assembled Monolayers of Bianchoring Ferrocene–Triazole Derivatives by "Click―Chemistry. Langmuir, 2022, 38, 3585-3596.	1.6	6
6	Biomolecular control over local gating in bilayer graphene induced by ferritin. IScience, 2022, 25, 104128.	1.9	1
7	Coherence Between Different Propagating Surface Plasmon Polariton Modes Excited by Quantum Mechanical Tunnel Junctions. Advanced Optical Materials, 2022, 10, .	3.6	3
8	Stable Universal 1―and 2â€Input Singleâ€Molecule Logic Gates. Advanced Materials, 2022, 34, e2202135.	11.1	10
9	Phase Matching via Plasmonic Modal Dispersion for Third Harmonic Generation. Advanced Science, 2022, 9, .	5.6	2
10	Interplay between Interfacial Energy, Contact Mechanics, and Capillary Forces in EGaIn Droplets. ACS Applied Materials & Interfaces, 2022, 14, 28074-28084.	4.0	6
11	The energy level alignment of the ferrocene–EGaln interface studied with photoelectron spectroscopy. Physical Chemistry Chemical Physics, 2021, 23, 13458-13467.	1.3	5
12	Switching of the mechanism of charge transport induced by phase transitions in tunnel junctions with large biomolecular cages. Journal of Materials Chemistry C, 2021, 9, 10768-10776.	2.7	6
13	Room-temperature tunnel magnetoresistance across biomolecular tunnel junctions based on ferritin. JPhys Materials, 2021, 4, 035003.	1.8	5
14	Silicon-Based Quantum Mechanical Tunnel Junction for Plasmon Excitation from Low-Energy Electron Tunneling. ACS Photonics, 2021, 8, 1951-1960.	3.2	11
15	Biasâ€Polarityâ€Dependent Direct and Inverted Marcus Charge Transport Affecting Rectification in a Redoxâ€Active Molecular Junction. Advanced Science, 2021, 8, e2100055.	5.6	14
16	A single atom change turns insulating saturated wires into molecular conductors. Nature Communications, 2021, 12, 3432.	5.8	16
17	Energy-Level Alignment and Orbital-Selective Femtosecond Charge Transfer Dynamics of Redox-Active Molecules on Au, Ag, and Pt Metal Surfaces. Journal of Physical Chemistry C, 2021, 125, 18474-18482.	1.5	2
18	Optical Anisotropy in van der Waals materials: Impact on Direct Excitation of Plasmons and Photons by Quantum Tunneling. Light: Science and Applications, 2021, 10, 230.	7.7	7

#	Article	IF	CITATIONS
19	Role of Order in the Mechanism of Charge Transport across Single-Stranded and Double-Stranded DNA Monolayers in Tunnel Junctions. Journal of the American Chemical Society, 2021, 143, 20309-20319.	6.6	19
20	Geometric Control Over the Edge Diffraction of Electrically Excited Surface Plasmon Polaritons by Tunnel Junctions. ACS Photonics, 2021, 8, 3591-3598.	3.2	2
21	Cavity Plasmonics in Tunnel Junctions: Outcoupling and the Role of Surface Roughness. Physical Review Applied, 2020, 14, .	1.5	12
22	Functional Redoxâ€Active Molecular Tunnel Junctions. Chemistry - an Asian Journal, 2020, 15, 3752-3770.	1.7	28
23	Design principles of dual-functional molecular switches in solid-state tunnel junctions. Applied Physics Letters, 2020, 117, .	1.5	20
24	Reversal of the Direction of Rectification Induced by Fermi Level Pinning at Molecule–Electrode Interfaces in Redox-Active Tunneling Junctions. ACS Applied Materials & Interfaces, 2020, 12, 55044-55055.	4.0	21
25	Large Increase in the Dielectric Constant and Partial Loss of Coherence Increases Tunneling Rates across Molecular Wires. ACS Applied Materials & Interfaces, 2020, 12, 45111-45121.	4.0	18
26	Solid-State Protein Junctions: Cross-Laboratory Study Shows Preservation of Mechanism at Varying Electronic Coupling. IScience, 2020, 23, 101099.	1.9	30
27	Electric-field-driven dual-functional molecular switches in tunnel junctions. Nature Materials, 2020, 19, 843-848.	13.3	124
28	Protective Layers Based on Carbon Paint To Yield High-Quality Large-Area Molecular Junctions with Low Contact Resistance. Journal of the American Chemical Society, 2020, 142, 3513-3524.	6.6	29
29	Self-Assembly and Electrochemical Characterization of Ferrocene-based Molecular Diodes for Solar Rectenna Device. MRS Advances, 2020, 5, 3185-3194.	0.5	3
30	Unraveling the Failure Modes of Molecular Diodes: The Importance of the Monolayer Formation Protocol and Anchoring Group to Minimize Leakage Currents. Journal of Physical Chemistry C, 2019, 123, 19759-19767.	1.5	11
31	Ultrasmooth and Photoresistâ€Free Microporeâ€Based EGaIn Molecular Junctions: Fabrication and How Roughness Determines Voltage Response. Advanced Functional Materials, 2019, 29, 1904452.	7.8	34
32	Interplay of Collective Electrostatic Effects and Level Alignment Dictates the Tunneling Rates across Halogenated Aromatic Monolayer Junctions. Journal of Physical Chemistry Letters, 2019, 10, 4142-4147.	2.1	25
33	Rectification Ratio and Tunneling Decay Coefficient Depend on the Contact Geometry Revealed by in Situ Imaging of the Formation of EGaln Junctions. ACS Applied Materials & Interfaces, 2019, 11, 21018-21029.	4.0	37
34	Directional Excitation of Surface Plasmon Polaritons via Molecular Through-Bond Tunneling across Double-Barrier Tunnel Junctions. Nano Letters, 2019, 19, 4634-4640.	4.5	21
35	The supramolecular structure and van der Waals interactions affect the electronic structure of ferrocenyl-alkanethiolate SAMs on gold and silver electrodes. Nanoscale Advances, 2019, 1, 1991-2002.	2.2	10
36	Molecular Electronic Plasmonics: In Operando Characterization and Control over Intermittent Light Emission from Molecular Tunnel Junctions via Molecular Backbone Rigidity (Adv. Sci. 20/2019). Advanced Science, 2019, 6, 1970122.	5.6	2

#	Article	IF	CITATIONS
37	Control over Near-Ballistic Electron Transport through Formation of Parallel Pathways in a Single-Molecule Wire. Journal of the American Chemical Society, 2019, 141, 240-250.	6.6	39
38	Molecular Diodes: Stable Molecular Diodes Based on π–π Interactions of the Molecular Frontier Orbitals with Graphene Electrodes (Adv. Mater. 10/2018). Advanced Materials, 2018, 30, 1870069.	11.1	0
39	Stable Molecular Diodes Based on π–π Interactions of the Molecular Frontier Orbitals with Graphene Electrodes. Advanced Materials, 2018, 30, 1706322.	11.1	35
40	A Black Phosphorus Carbide Infrared Phototransistor. Advanced Materials, 2018, 30, 1705039.	11.1	95
41	Transition from direct to inverted charge transport Marcus regions in molecular junctions via molecular orbital gating. Nature Nanotechnology, 2018, 13, 322-329.	15.6	98
42	Bottom-electrode induced defects in self-assembled monolayer (SAM)-based tunnel junctions affect only the SAM resistance, not the contact resistance or SAM capacitance. RSC Advances, 2018, 8, 19939-19949.	1.7	9
43	Enhancing Reproducibility and Nonlocal Effects in Film oupled Nanoantennas. Advanced Optical Materials, 2018, 6, 1801177.	3.6	5
44	The Drive Force of Electrical Breakdown of Largeâ€Area Molecular Tunnel Junctions. Advanced Functional Materials, 2018, 28, 1801710.	7.8	28
45	Molecular Electronics: The Drive Force of Electrical Breakdown of Large-Area Molecular Tunnel Junctions (Adv. Funct. Mater. 28/2018). Advanced Functional Materials, 2018, 28, 1870192.	7.8	1
46	Molecular Coatings for Stabilizing Silver and Gold Nanocubes under Electron Beam Irradiation. Langmuir, 2017, 33, 1189-1196.	1.6	14
47	Tuning the Rectification Ratio by Changing the Electronic Nature (Open-Shell and Closed-Shell) in Donor–Acceptor Self-Assembled Monolayers. Journal of the American Chemical Society, 2017, 139, 4262-4265.	6.6	51
48	Supramolecular Structure of the Monolayer Triggers Odd–Even Effects in the Tunneling Rates across Noncovalent Junctions on Graphene. Journal of Physical Chemistry C, 2017, 121, 4172-4180.	1.5	15
49	Fabrication of ultra-smooth and oxide-free molecule-ferromagnetic metal interfaces for applications in molecular electronics under ordinary laboratory conditions. RSC Advances, 2017, 7, 14544-14551.	1.7	9
50	Highly efficient on-chip direct electronic–plasmonic transducers. Nature Photonics, 2017, 11, 623-627.	15.6	124
51	Robust resistive memory devices using solution-processable metal-coordinated azoÂaromatics. Nature Materials, 2017, 16, 1216-1224.	13.3	244
52	Surface and buried interface layer studies on challenging structures as studied by ARXPS. Surface and Interface Analysis, 2017, 49, 1309-1315.	0.8	40
53	Molecular diodes with rectification ratios exceeding 105 driven by electrostatic interactions. Nature Nanotechnology, 2017, 12, 797-803.	15.6	224
54	Multistep nucleation of nanocrystals in aqueous solution. Nature Chemistry, 2017, 9, 77-82.	6.6	312

#	Article	IF	CITATIONS
55	Real-Time Dynamics of Galvanic Replacement Reactions of Silver Nanocubes and Au Studied by Liquid-Cell Transmission Electron Microscopy. ACS Nano, 2016, 10, 7689-7695.	7.3	67
56	Functionalized 1â€2-Substituted Iodoferrocenes and Their Pd-Catalyzed Heck Cross-Coupling Reactions. European Journal of Inorganic Chemistry, 2016, 2016, 1314-1318.	1.0	9
57	Electrostatic control over temperature-dependent tunnelling across a single-molecule junction. Nature Communications, 2016, 7, 11595.	5.8	35
58	Separation of superparamagnetic particles through ratcheted Brownian motion and periodically switching magnetic fields. Biomicrofluidics, 2016, 10, 064105.	1.2	4
59	Charge Transport: Longâ€Range Tunneling Processes across Ferritinâ€Based Junctions (Adv. Mater. 9/2016). Advanced Materials, 2016, 28, 1900-1900.	11.1	1
60	Comparison of DC and AC Transport in 1.5–7.5 nm Oligophenylene Imine Molecular Wires across Two Junction Platforms: Eutectic Ga–In versus Conducting Probe Atomic Force Microscope Junctions. Journal of the American Chemical Society, 2016, 138, 7305-7314.	6.6	64
61	Molecular Electronics: Noncovalent Selfâ€Assembled Monolayers on Graphene as a Highly Stable Platform for Molecular Tunnel Junctions (Adv. Mater. 4/2016). Advanced Materials, 2016, 28, 784-784.	11.1	3
62	Real-Time Imaging of the Formation of Au–Ag Core–Shell Nanoparticles. Journal of the American Chemical Society, 2016, 138, 5190-5193.	6.6	55
63	Supramolecular vs Electronic Structure: The Effect of the Tilt Angle of the Active Group in the Performance of a Molecular Diode. Journal of the American Chemical Society, 2016, 138, 5769-5772.	6.6	49
64	Even the Odd Numbers Help: Failure Modes of SAM-Based Tunnel Junctions Probed via Odd-Even Effects Revealed in Synchrotrons and Supercomputers. Accounts of Chemical Research, 2016, 49, 2061-2069.	7.6	68
65	Temperature dependent charge transport across tunnel junctions of single-molecules and self-assembled monolayers: a comparative study. Dalton Transactions, 2016, 45, 17153-17159.	1.6	22
66	Charge transfer plasmon resonances across silver–molecule–silver junctions: estimating the terahertz conductance of molecules at near-infrared frequencies. RSC Advances, 2016, 6, 70884-70894.	1.7	17
67	A Single-Level Tunnel Model to Account for Electrical Transport through Single Molecule- and Self-Assembled Monolayer-based Junctions. Scientific Reports, 2016, 6, 26517.	1.6	70
68	Chemical control over the energy-level alignment in a two-terminal junction. Nature Communications, 2016, 7, 12066.	5.8	50
69	Noncovalent Selfâ€Assembled Monolayers on Graphene as a Highly Stable Platform for Molecular Tunnel Junctions. Advanced Materials, 2016, 28, 631-639.	11.1	48
70	Longâ€Range Tunneling Processes across Ferritinâ€Based Junctions. Advanced Materials, 2016, 28, 1824-1830.	11.1	79
71	On-chip molecular electronic plasmon sources based on self-assembled monolayer tunnel junctions. Nature Photonics, 2016, 10, 274-280.	15.6	110
72	Tuning the Tunneling Rate and Dielectric Response of SAMâ€Based Junctions via a Single Polarizable Atom. Advanced Materials, 2015, 27, 6689-6695.	11.1	34

#	Article	IF	CITATIONS
73	Defect Scaling with Contact Area in EGaIn-Based Junctions: Impact on Quality, Joule Heating, and Apparent Injection Current. Journal of Physical Chemistry C, 2015, 119, 960-969.	1.5	56
74	Controlling the direction of rectification in a molecular diode. Nature Communications, 2015, 6, 6324.	5.8	197
75	Probing the nature and resistance of the molecule–electrode contact in SAM-based junctions. Nanoscale, 2015, 7, 12061-12067.	2.8	28
76	A Molecular Diode with a Statistically Robust Rectification Ratio of Three Orders of Magnitude. Nano Letters, 2015, 15, 5506-5512.	4.5	118
77	The Origin of the Odd–Even Effect in the Tunneling Rates across EGaln Junctions with Self-Assembled Monolayers (SAMs) of <i>n</i> -Alkanethiolates. Journal of the American Chemical Society, 2015, 137, 10659-10667.	6.6	63
78	Odd–Even Effects in Charge Transport through Self-Assembled Monolayer of Alkanethiolates. Journal of Physical Chemistry C, 2015, 119, 5657-5662.	1.5	29
79	Electrically-Excited Surface Plasmon Polaritons with Directionality Control. ACS Photonics, 2015, 2, 385-391.	3.2	34
80	Fabrication of ultra-flat silver surfaces with sub-micro-meter scale grains. Thin Solid Films, 2015, 593, 26-39.	0.8	18
81	Arrays of high quality SAM-based junctions and their application in molecular diode based logic. Nanoscale, 2015, 7, 19547-19556.	2.8	38
82	One-Nanometer Thin Monolayers Remove the Deleterious Effect of Substrate Defects in Molecular Tunnel Junctions. Nano Letters, 2015, 15, 6643-6649.	4.5	50
83	Reversible Soft Topâ€Contacts to Yield Molecular Junctions with Precise and Reproducible Electrical Characteristics. Advanced Functional Materials, 2014, 24, 4442-4456.	7.8	84
84	Giant enhancement in vertical conductivity of stacked CVD graphene sheets by self-assembled molecular layers. Nature Communications, 2014, 5, 5461.	5.8	83
85	Bias induced transition from an ohmic to a non-ohmic interface in supramolecular tunneling junctions with Ga <sub>2</sub> O <sub>3</sub> /EGaIn top electrodes. Nanoscale, 2014, 6, 11246-11258.	2.8	41
86	Controlling Leakage Currents: The Role of the Binding Group and Purity of the Precursors for Self-Assembled Monolayers in the Performance of Molecular Diodes. Journal of the American Chemical Society, 2014, 136, 1982-1991.	6.6	83
87	On the Remarkable Role of Surface Topography of the Bottom Electrodes in Blocking Leakage Currents in Molecular Diodes. Journal of the American Chemical Society, 2014, 136, 6554-6557.	6.6	98
88	Equivalent Circuits of a Self-Assembled Monolayer-Based Tunnel Junction Determined by Impedance Spectroscopy. Journal of the American Chemical Society, 2014, 136, 11134-11144.	6.6	94
89	Dependency of the Tunneling Decay Coefficient in Molecular Tunneling Junctions on the Topography of the Bottom Electrodes. Angewandte Chemie - International Edition, 2014, 53, 3377-3381.	7.2	78
90	Encapsulated Annealing: Enhancing the Plasmon Quality Factor in Lithographically–Defined Nanostructures. Scientific Reports, 2014, 4, 5537.	1.6	96

#	Article	IF	CITATIONS
91	Electrical Resistance of Ag <sup>TS</sup> –S(CH <sub>2</sub> ) <sub><i>n</i>â^'1</sub> CH <sub>3</sub> //Ga <sub>2</sub> O <sub>3 Tunneling Junctions. Journal of Physical Chemistry C, 2012, 116, 10848-10860.</sub>	<b su5b>/EC	Gal <b>1</b> 97
92	Statistical Tools for Analyzing Measurements of Charge Transport. Journal of Physical Chemistry C, 2012, 116, 6714-6733.	1.5	109
93	The SAM, Not the Electrodes, Dominates Charge Transport in Metal-Monolayer//Ga <sub>2</sub> O <sub>3</sub> /Gallium–Indium Eutectic Junctions. ACS Nano, 2012, 6, 4806-4822.	7.3	130
94	A Molecular Half-Wave Rectifier. Journal of the American Chemical Society, 2011, 133, 15397-15411.	6.6	102
95	Luminescent acetylthiol derivative tripodal osmium(II) and iridium(III) complexes: Spectroscopy in solution and on surfaces. Pure and Applied Chemistry, 2011, 83, 779-799.	0.9	11
96	Mechanism of Rectification in Tunneling Junctions Based on Molecules with Asymmetric Potential Drops. Journal of the American Chemical Society, 2010, 132, 18386-18401.	6.6	205
97	Charge Transport and Rectification in Arrays of SAM-Based Tunneling Junctions. Nano Letters, 2010, 10, 3611-3619.	4.5	213
98	Molecular Rectification in Metalâ ``SAMâ ``Metal Oxideâ ``Metal Junctions. Journal of the American Chemical Society, 2009, 131, 17814-17827.	6.6	257
99	Preparation of metal–SAM–dendrimer–SAM–metal junctions by supramolecular metal transfer printing. New Journal of Chemistry, 2008, 32, 652.	1.4	11
100	Redox-Controlled Interaction of Biferrocenyl-Terminated Dendrimers with β-Cyclodextrin Molecular Printboards. Chemistry - A European Journal, 2007, 13, 69-80.	1.7	47
101	Controlling the Supramolecular Assembly of Redox-Active Dendrimers at Molecular Printboards by Scanning Electrochemical Microscopy. Langmuir, 2006, 22, 9770-9775.	1.6	60
102	Room-Temperature Single-Electron Tunneling in Dendrimer-Stabilized Gold Nanoparticles Anchored at a Molecular Printboard. Small, 2006, 2, 1422-1426.	5.2	24
103	Multivalent Dendrimers at Molecular Printboards:  Influence of Dendrimer Structure on Binding Strength and Stoichiometry and Their Electrochemically Induced Desorption. Langmuir, 2005, 21, 7866-7876.	1.6	85
104	Binding Control and Stoichiometry of Ferrocenyl Dendrimers at a Molecular Printboard. Journal of the American Chemical Society, 2004, 126, 12266-12267.	6.6	119